Acta of Bioengineering and Biomechanics
Vol. 13, No. 2, 2011

Original paper

Motion synthesis and force distribution analysis for a biped robot

MACIEJ T. TROJNACKI[1]*, TERESA ZIELIŃSKA[2]

[1] Industrial Research Institute for Automation and Measurements (PIAP), Warsaw, Poland.
[2] Institute of Aeronautics and Applied Mechanics (ITLiMS), Warsaw University of Technology, Warsaw, Poland.

In this paper, the method of generating biped robot motion using recorded human gait is presented. The recorded data were modified taking into account the velocity available for robot drives. Data includes only selected joint angles, therefore the missing values were obtained considering the dynamic postural stability of the robot, which means obtaining an adequate motion trajectory of the so-called Zero Moment Point (ZMT). Also, the method of determining the ground reaction forces' distribution during the biped robot's dynamic stable walk is described. The method was developed by the authors. Following the description of equations characterizing the dynamics of robot's motion, the values of the components of ground reaction forces were symbolically determined as well as the coordinates of the points of robot's feet contact with the ground. The theoretical considerations have been supported by computer simulation and animation of the robot's motion. This was done using Matlab/Simulink package and Simulink 3D Animation Toolbox, and it has proved the proposed method.

Key words: *biped robot, motion synthesis, dynamic equilibrium, ground reaction forces' distribution, computer simulation*

1. Introduction

Nowadays, a very intense development of the walking robots is observed, especially the biped ones. Intensified research on such robots is carried out in the Far East countries. Attempts to construct a humanoid robot are being made (Honda ASIMO, Sony QRIO), as well as to build machines dedicated to supplementing a traditional wheel-chair with a walking mechanism. Resultant motion of machines such as Waseda WL-16R, Toyota iFoot, KAIST Hubo FX-1 is controlled by a human.

Most of the biped robots are dedicated to education and research, or produced for entertainment. Some of the humanoid robots, like Honda ASIMO [1], are designed to be personal, for example, to help elderly or disabled people.

Due to many reasons, designing the walking robots is a very challenging task. One of the basic problems is the motion synthesis, which in the case of discreet locomotion is considerably more difficult, when compared to the continuous one. Researchers usually obtain biped robots' motion pattern by applying the zero moment point (ZMP) criterion [1], [2], [3]–[8], in which the inverse kinematics problem must be solved. But this produces the theoretical problem when solving the inverse kinematics to obtain the control signals. For fully straightened leg a singular configuration occurs. This results in biped robots moving with their legs slightly bent to avoid the singular position. But this is not typical of a walking human. Moreover, the movement of the robot with bent legs decreases its energetic efficiency. For these reasons generation of the motion of such robots using the biological patterns, and especially the recorded human gait [9], is justified. In the paper [10], the method for the synthesis of the biped robot's walk, without the necessity to solve the inverse kinematics problem, has been pre-

* Corresponding author: Maciej T. Trojnacki, Industrial Research Institute for Automation and Measurements (PIAP), Al. Jerozolimskie 202, 02-486 Warsaw, Poland. E-mail: mtrojnacki@piap.pl

Received: May 28th, 2010
Accepted for publication: March 29th, 2011

sented. The method refers to the concepts of the biological generators of the motion rhythm.

The analysis of the ground reaction forces' distribution (or the forces exerted by robot's legs on the ground) is important for determining the robot's postural stability as well as for the synthesis of position-force control. Such an analysis is a difficult issue. The gait phase with only one leg of the robot touching the ground is the simplest to study it. The robot and the ground form an open kinematic chain, hence the searched values can be explicitly determined. This issue becomes more complicated, when more than one leg touches the ground. In that case, the robot's legs and the ground form a closed kinematic chains, and unique solution cannot be given. This is the case where two legs of the biped robot are touching the ground (it is double support phase of the gait). Motion of the four-legged robots walking diagonally is also the example of that situation. In such a case, where the feet touch the ground at a point of contact basis, there are six unknown components of the ground reaction forces (or the forces exerted by robot's legs on the ground) to be determined and six dynamic motion equations can be formulated. However, those equations are singular (matrix rank does not exceeds five). If the robot has legs ending with feet, the leg-end ground contact is not the point but some area (the foothold). Then, the application points of the resultant reaction forces' vectors acting on each foot have to be determined. The determination of the ground reaction forces' distribution (or the forces exerted by robot's legs on the ground) is even more complicated for multi-legged robots (with six or more legs). Here, more forces (and their application points) require determination. But the number of dynamic motion equations remains still equal to six.

There are not many examples in the literature giving the analysis of the ground reaction forces' distribution during the biped robot's walk. Synthesis of the robot's motion using mainly ZMP criterion is described more often. Other methods, mainly biologically inspired, are described, e.g., in paper [9].

In the approach based on the experiments, the researchers record the ground reaction forces, focusing on their vertical components. The works, where the authors are evaluating the localization of the resultant point contacts of the robot's foot with the ground, are very rare.

In the study [11], the authors focus on the synthesis of the robot's motion, based on the earlier simulation with the OpenHRP platform. Both the simulation and the experiments are used to determine the vertical components of the ground reaction forces. The foot mechanism is expressed as springs–dampers system. This system allows us to reduce the effect of the foot impact during touch-down.

In the study [12], the authors describe the control system, developed for a running biped robot. Robot controller includes several functional parts responsible for different actions, one of those is stabilization of the robot's posture, other are: absorption of impacts of the foot on the ground and control of vertical components for the leg-end forces. Authors implemented this method in the running robot. Robot moves on significantly bent legs, which is not typically observed for a running human. In a such posture, for the realisation of the robot's motion, the high values of the driving torques are required. Paper [13] is devoted to a similar problem, but additionally the robot's capability to jump is described.

Authors of the study [14] present the motion control for three different biped robots, using the results obtained in passive walking analysis. Such an approach allows us to perform the walk with smaller energy consumption than during the motion synthetized using the other methods mentioned above. Authors also registered the vertical components of the ground reaction forces expressed in the reference frame attached accordingly to the robot's leg.

The authors of this paper have studied the ground reaction forces' distribution for the four-legged robots, which has been described in [15]–[18].

Here, the method of biped robot motion synthesis using the pattern of a human gait is introduced. The recorded data were modified, taking into account the speed achievable by the robot drives. Only joint angles in hip and knee joints were given, therefore the identification of motion phases had to be done. The determination of the remaining quantities, essential for the realization of the robot's motion, was also needed. Joint angles in the remaining robot's joints were determined in order to assure the robot's dynamic equilibrium. Changes (during the walk) of the robot's centre of gravity (CG) and position of zero moment point (ZMP) were calculated, taking into account the dimensions and mass parameters of the robot.

The distribution of the ground reaction forces, described in this paper, was determined in a way similar to that as in studies [16]–[18]. The main difference in the solution proposed hereby results from different design of the robot feet. Research described in studies [16]–[18] was focused on the robot with circular feet, equipped with three passive degrees of freedom, which gives the capability of making two independent rotations and one translation limited by the spring. In

the solution presented hereby, the robot has one active degree of freedom in the ankle and one passive degree of freedom due to the spring embedded in the foot.

In order to verify the method developed, the simulation tests were performed, using Matlab/Simulink package. The animation of the robot's motion has been made with the Simulink 3D Animation Toolbox, with the aim to visually verify the correctness of generated motion.

2. Data describing human gait

Data describing human gait, presented in this paper, were collected by the authors of the publication [10]. Time characteristics of the joint angles in hip joints and knee joints (figure 1) were recorded during the human walk.

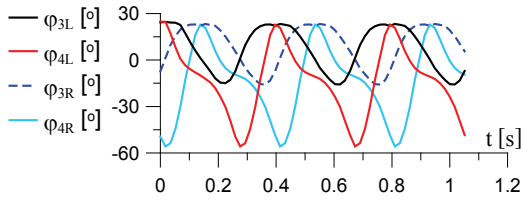

Fig. 1. Results of the human gait recording [10]: joint angles in hips (φ_{3L}, φ_{3R}) and knees (φ_{4L}, φ_{4R}) (L – left leg, R – right leg)

It is assumed that the joint angles are expressed in reference to the vertical lines. When the segment of the leg protrudes forward towards the vertical line attached to the appropriate joint it constitutes a positive angle, in the backward – it is a negative angle, and in the case of overlapping – a zero one. Data were recorded with the constant frequency of 58 packets per second.

3. Biped robot

3.1. Kinematic structure

Robot described in this paper has twelve degrees of freedom. The construction of the robot was described in [19]. Each leg has 6 active degrees of freedom: 3 in the hip joint, 1 in the knee and 2 in the ankle joint. Such a structure of the leg enables realisation of the motion similar to the human one. Legs of the robot are ended with rectangle-shaped feet.

The kinematic structure of the robot is shown in figure 2, including the notation of the robot's segments, specific points, and angles used to define the orientation of the body, coordinate system attached to the body, as well as joint angles of the robot's leg. Also the important dimensions of the robot have been marked.

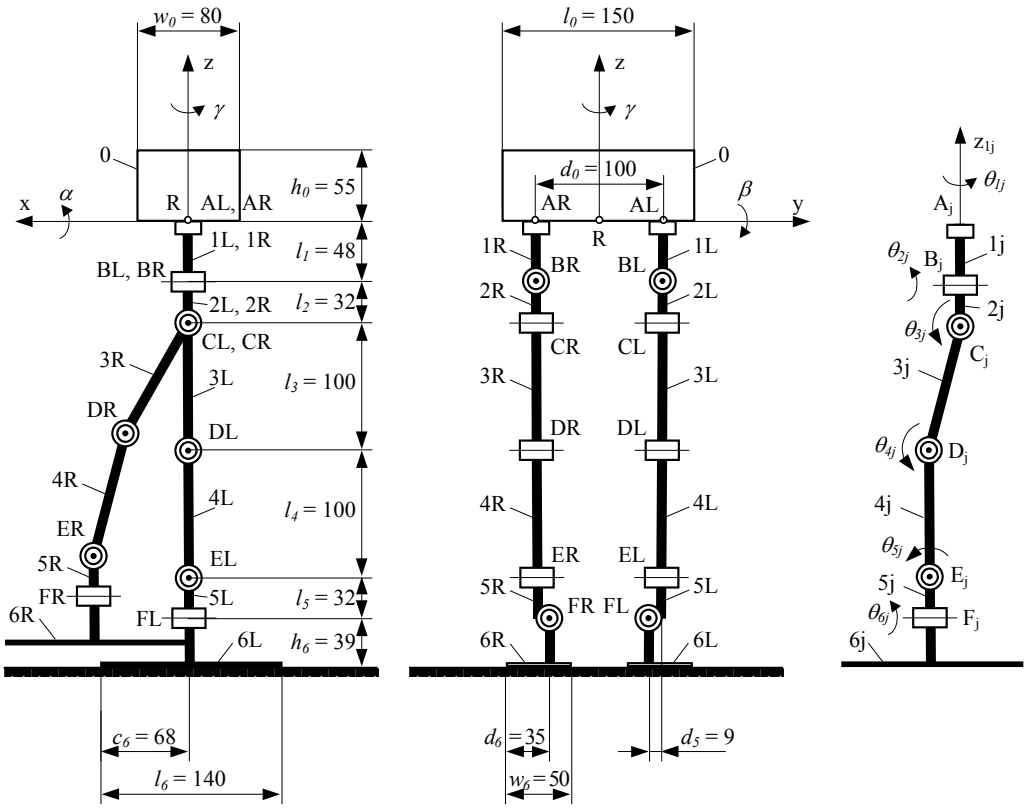

Fig. 2. Kinematic structure of the robot with important dimensions and markings of the joint angles for j-leg [18]

3.2. Notation

The following coordinate systems were defined: *OXYZ* – non-moving reference frame, *RXYZ* frame attached to the body (figure 2). It has been assumed that in the starting point the axes of both frames overlap (both systems are oriented identically). The superscript on the left side of the symbol denotes the reference frame in which that value is expressed. The subscript on the right side of the symbol specifies the coordinate (x, y, z) of the leg and (if applicable) the number of leg segment. Symbol i denotes the number of the consecutive leg segments (i = 1, ..., 6), each leg is noted by $j = \{L, R\}$ index, where L is for the left and R is for the right legs.

For example, ${}^{O}v_{AL}$ denotes the value v expressed in *OXYZ* system, applied in *AL* point, i.e., in *A* point of the leg.

3.3. Construction of the robot

The robot was designed using the Unigraphics software (figure 3) [20]. It was equipped with technologically advanced Dynamixel DX-113 and DX-116 servo-drives.

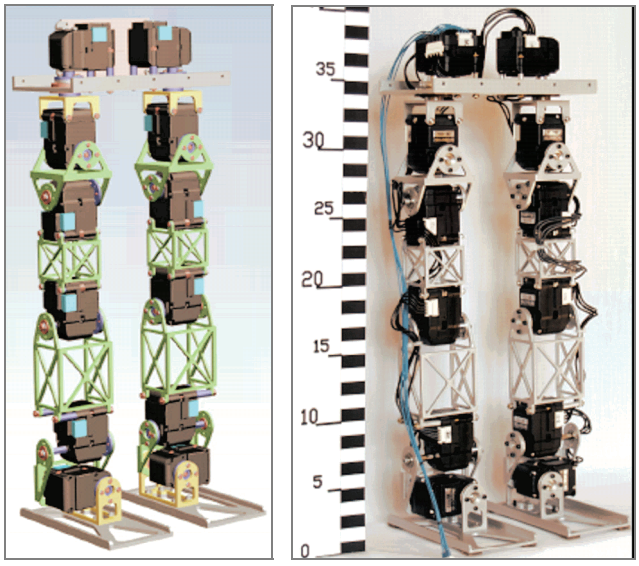

Fig. 3. The robot designed in the Unigraphics and the actual construction [19]

On the basis of the Unigraphics design, the mass parameters of the robot were obtained and taken into account during the simulation tests. Total mass of the robot equals ca. m = 1.5 [kg], masses of the particular segments equal accordingly: body, m_0 = 0.363 [kg], upper part of the hip, m_1 = 0.096 [kg], lower part of the hip, m_2 = 0.013 [kg], thigh, m_3 = 0.171 [kg], shin, m_4 = 0.103 [kg], ankle, m_5 = 0.092 [kg], foot, m_6 = 0.101 [kg].

The development of the new design of the foot, with springs mounted in it, has been launched. This will enable additional susceptibility of the foot, and ensure a moderate transition from the support phase to the transfer phase and back. Specially designed latch mechanism will also enable energy accumulation during the support phase and its usage at the moment of transfer phase initialization.

4. Generation of the biped robot's motion

4.1. Transformation of the recorded angles into joint angles of the robot

Before the robot's motion generation, the transformation of the joint angles, recorded during human gait, into the joint angles considered in the model of the robot was performed. The following dependencies are valid:

$$\begin{aligned} &\theta_{3j} = -\varphi_{3j}, \quad \theta_{4j} = \varphi_{3j} - \varphi_{4j}, \\ &\theta_{5j} = -\theta_{3j} - \theta_{4j}, \quad j = \{L, R\}. \end{aligned} \tag{1}$$

As a result, 6 joint angles were obtained. It was initially assumed that during the robot's motion its feet orientation would not be changed in reference to the body. In this paper, only the forward motion of the robot is analyzed, therefore only generation of the four angles in the legs and feet was necessary. To indentify the relationship between the joint angular trajectories and the angular velocities needed for robot's drives, the step time has been modified, compared to the one used in human gait, to the value dt = 0.08 [s]. This means that the time frames have been changed in a 1:4.64 ratio. As a result of this transformation, joint angles and modified velocities of the joints were obtained.

4.2. Determination of the motion phases

Identification of the transfer and support phases of a given leg, as well as of the motion trajectory of the body R point, is possible, using the determined joint angles $\theta_{3j} - \theta_{5j}$ of the robot. The specific phases of the

robot's motion can be identified via the analysis of the *Fj* points coordinates, in the reference frame connected with the robot's body, by using the following dependencies:

$$^{R}x_{Fj} = -l_2 s_{1j} s_{2j} - l_3(c_{1j} s_{3j} + s_{1j} s_{2j} c_{3j}) - l_4(c_{1j} s_{34j} + s_{1j} s_{2j} c_{34j}) - l_5(c_{1j} s_{345j} + s_{1j} s_{2j} c_{345j}), \tag{2a}$$

$$^{R}y_{Fj} = \pm d_0/2 \pm l_2 c_{1j} s_{2j} - l_3(s_{1j} s_{3j} - c_{1j} s_{2j} c_{3j}) - l_4(s_{1j} s_{34j} - c_{1j} s_{2j} c_{34j}) - l_5(s_{1j} s_{345j} + c_{1j} s_{2j} c_{345j}), \tag{2b}$$

$$^{R}z_{Fj} = -l_1 - l_2 c_{2j} - l_3 c_{2j} c_{3j} - l_4 c_{2j} c_{34j} - l_5 c_{2j} c_{345j}, \tag{2c}$$

where: $s_{ij} = \sin\theta_{ij}$, $c_{ij} = \cos\theta_{ij}$, $s_{34j} = \sin(\theta_{3j} + \theta_{4j})$, $c_{34j} = \cos(\theta_{3j} + \theta_{4j})$, $s_{345j} = \sin(\theta_{3j} + \theta_{4j} + \theta_{5j})$, $c_{345j} = \cos(\theta_{3j} + \theta_{4j} + \theta_{5j})$.

For $j = L$ in equation (2b) the mark ± should be taken as "+", and for $j = R$ as "–".

Based on the calculated time frames of the *Fj* points' coordinates, the phases of the robot's motion, connected with the transfer and support of each leg, were determined.

4.3. Dynamic equilibrium

The method for the dynamic equilibrating of the robot's posture was developed based on the identification of motion phases as well as on the values of joint angles $\theta_{3j} - \theta_{5j}$. It was assumed that robot's body was being laterally translated (when there was no inclination $\alpha = 0$), and that the joint angle θ_{2j} depended on the joint angle θ_{6j} as follows:

$$\theta_{2j} = -\theta_{6j}. \tag{3}$$

These angles were generated in such a manner as to ensure the dynamic balancing of the robot, i.e., to have the zero moment point following the right trajectory.

This assumption is accepted to obtain the maximum inclination in the middle of the double support phase. Transition from one extreme inclination to another should be done by slight modifications during some period of time. The θ_{2j} and θ_{6j} angles may be sinusoidal in shape, and their amplitude should be chosen for the zero moment point to be located within the foothold of the leg, which in a next time instant will be the only one support during the maximum lateral inclination. As a result of the dynamic equilibration, the motion trajectory of the points *Fj* will be modified.

4.4. Location of the centre of gravity and the zero moment point

In order to verify the method assumed for the dynamic equilibration, the changes of the centre of gravity and zero moment point coordinates during the motion were calculated.

The centre of gravity coordinates (CG) in the *RXYZ* system is calculated using the following dependence:

$$^{R}w_{CG} = \frac{m_0\,^{R}w_0 + \sum_i \sum_j m_i\,^{R}w_{ij}}{m}, \tag{4}$$

where: i – number of robot segments in the leg (i = 1, ..., 6), $j = \{L, R\}$ – notation used to mark the leg, $^{R}w_0$, $^{R}w_{ij}$ – centre of gravity coordinate, $w = \{x, y, z\}$, m_0 – mass of the trunk (corpus), m_i – mass of the segment i of the leg (left or right), m – total mass of the robot.

Zero moment point (ZMP) has two interpretations [8]. One of them defines it as a point on the ground at which the net moment due to the inertial forces and the gravity forces has no component along the horizontal axes. According to the second definition, the zero moment point is the point at which the horizontal components of the moments generated by reaction force and reaction torque are equal to 0. In fact, both definitions are equal.

If the zero moment point is within the support area, the robot posture is stable, that means there is no rotation in reference to the edge of the foot.

ZMP coordinates can be calculated according to the first interpretation, using the following equations:

$$^{R}x_{\mathrm{ZMP}} = \frac{m_0(^{R}\ddot{z}_0 - {}^{R}g_Z)\,^{R}x_0 + \sum_i \sum_j m_i(^{R}\ddot{z}_{ij} - {}^{R}g_Z)\,^{R}x_{ij} - m_0\,^{R}\ddot{x}_0\,^{O}z_0 - \sum_i \sum_j m_i\,^{R}\ddot{x}_{ij}\,^{O}z_{ij}}{m_0(^{R}\ddot{z}_0 - {}^{R}g_Z) + \sum_i \sum_j m_i(^{R}\ddot{z}_{ij} - {}^{R}g_Z)}, \tag{5a}$$

$$^{R}y_{\mathrm{ZMP}} = \frac{m_0(^{R}\ddot{z}_0 - {}^{R}g_Z)\,^{R}y_0 + \sum_i \sum_j m_i(^{R}\ddot{z}_{ij} - {}^{R}g_Z)\,^{R}y_{ij} - m_0\,^{R}\ddot{y}_0\,^{O}z_0 - \sum_i \sum_j m_i\,^{R}\ddot{y}_{ij}\,^{O}z_{ij}}{m_0(^{R}\ddot{z}_0 - {}^{R}g_Z) + \sum_i \sum_j m_i(^{R}\ddot{z}_{ij} - {}^{R}g_Z)}, \tag{5b}$$

where: ${}^{R}\ddot{w}_0$, ${}^{R}\ddot{w}_{ij}$ – accordant components of the centre of mass acceleration of the body or the segment i of the leg j, ${}^{R}g$ – acceleration due to gravity, given in the reference frame of the robot's body.

If the coordinates of the CG point are known, ZMP coordinates can be also calculated using the following equations:

$$\begin{aligned} {}^{R}x_{\mathrm{ZMP}} &= {}^{R}x_{\mathrm{CG}} - \frac{{}^{R}\ddot{x}_{\mathrm{CG}}}{{}^{R}\ddot{z}_{\mathrm{CG}} - {}^{R}g_Z}\,{}^{O}z_{\mathrm{CG}}, \\ {}^{R}y_{\mathrm{ZMP}} &= {}^{R}y_{\mathrm{CG}} - \frac{{}^{R}\ddot{y}_{\mathrm{CG}}}{{}^{R}\ddot{z}_{\mathrm{CG}} - {}^{R}g_Z}\,{}^{O}z_{\mathrm{CG}}. \end{aligned} \tag{6}$$

Similar dependencies for the calculation of the ZMP can be found in [2], however, with exclusion of the acceleration ${}^{R}\ddot{z}_{\mathrm{CG}}$.

4.5. Kinematics of the specific points of the robot

On the basis of the robot's motion phases and joint angles, the change of the robot's specific points' coordinates in the absolute reference frame was determined. This was necessary for the animation of the robot's motion, which enabled the visual verification of the generated motion.

The algorithm for calculating the robot's specific points in the non-moving reference frame is based on the assumption that the supported foot does not change its location in this frame. This enables determination of the remaining coordinates of the robot's points in the non-moving reference frame, using motion phases and joint angles.

The following algorithm was applied for calculations:

1. Initially the body of the robot is not inclined to any side, nor rotated ($\alpha = 0$, $\beta = 0$, $\gamma = 0$). The coordinates of the R, $Fs1$ and $Fs2$ points ($s1 = \{L, R\}$ – supported leg, $s2 = \{R, L\}$ – second leg) in the absolute reference frame are initially known and equal to:

$${}^{O}x_R = 0,\quad {}^{O}y_R = 0,\quad {}^{O}z_R = h_6 - {}^{R}z_{Fs1},\quad {}^{O}x_{Fs1} = {}^{R}x_{Fs1},$$

$${}^{O}x_{Fs2} = {}^{R}x_{Fs2},\quad {}^{O}z_{Fs1} = h_6,\quad {}^{O}z_{Fs2} = {}^{O}z_R + {}^{R}z_{Fs2}.$$

If

$${}^{R}z_{FL} \le {}^{R}z_{FR},$$

then:

$$s1 = L,\ s2 = R,\quad {}^{O}y_{Fs1} = d_0/2,\quad {}^{O}y_{Fs2} = -d_0/2,$$

in other case:

$$s1 = R,\ s2 = L,\quad {}^{O}y_{Fs1} = -d_0/2,\quad {}^{O}y_{Fs2} = d_0/2.$$

2. In the following steps, the coordinates of the R point of the trunk (corpus) in the absolute reference frame are calculated as (in a given case of robot's forward movement $\gamma = 0$):

$${}^{O}x_R = {}^{O}x_{Fs1} - {}^{R}x_{Fs1}\cos\gamma + {}^{R}y_{Fs1}\sin\gamma,$$

$${}^{O}y_R = {}^{O}y_{Fs1} - {}^{R}x_{Fs1}\sin\gamma - {}^{R}y_{Fs1}\cos\gamma,$$

$${}^{O}z_R = {}^{O}z_{Fs1} - {}^{R}z_{Fs1}.$$

3. Taking into account the coordinates of the R point in the non-moving reference frame, the trunk (corpus) orientation and joint angles of the second leg, the coordinates of the $Fs2$ point ($s2 = \{R, L\}$) of the second leg (supported and transferred) in the absolute reference frame are calculated using the following dependencies:

$${}^{O}x_{Fs2} = {}^{O}x_R + {}^{R}x_{Fs2}\cos\gamma \_ {}^{R}y_{Fs2}\sin\gamma,$$

$${}^{O}y_{Fs2} = {}^{O}y_R + {}^{R}x_{Fs2}\sin\gamma + {}^{R}y_{Fs2}\cos\gamma,$$

$${}^{O}z_{Fs2} = {}^{O}z_R + {}^{R}z_{Fs2}.$$

4. Calculations from points 2–3 are repeated until the end of the support phase of the first leg. Equations for R, $Fs1$ and $Fs2$ points in absolute reference frame depicted in 1–3 points result from the transformation of these known coordinates in robot reference frame into absolute reference frame.

5. The next assumption is that the previously second leg becomes the first one (supported); and adequately the previously first leg becomes the second one (which was supported before) and the calculations are repeated from point 2 until the end of the robot's motion.

5. Ground reaction forces' distribution

5.1. Model of the robot dynamics

Equations for the robot dynamics in the $RXYZ$ reference frame attached to the robot's trunk (corpus) are obtained by applying the Newton–Euler formalism [21]:

$$m\,{}^{R}\ddot{\mathbf{r}}_{\mathrm{CG}} = -\sum_k {}^{R}\mathbf{F}_k + m\,{}^{R}\mathbf{g}, \tag{7}$$

$$\mathbf{I}^*\ddot{\mathbf{q}} + \dot{\mathbf{q}} \times \mathbf{I}^*\dot{\mathbf{q}} = -\sum_k ({}^R\mathbf{r}_k \times {}^R\mathbf{F}_k) + {}^R\mathbf{r}_{\mathrm{CG}} \times m\,{}^R\mathbf{g}\,, \quad (8)$$

where: k – (subscript) denotes the supporting leg, ${}^R\mathbf{F}_k$ – force exerted by the k-th leg on the ground, ${}^R\mathbf{R}_k = -{}^R\mathbf{F}_k$ – reaction force acting on that leg, ${}^R\mathbf{r}_{\mathrm{CG}}$, ${}^R\mathbf{r}_k$ – vectors determining location of the robot's centre of gravity and point at which reaction force acts on the k-th leg, ${}^R\mathbf{g}$ – gravity vector, ${}^R\ddot{\mathbf{r}}_{\mathrm{CG}}$ – vector of the absolute acceleration of the robot's centre of gravity, $\mathbf{I}^*$ – inertia tensor calculated for $RXYZ$ reference frame based on the known inertia tensor $\mathbf{I}$ of the robot and using parallel axis theorem [21], $\mathbf{q}$ – vector of the angles of inclination, slope and rotation of the robot's body.

In this paper, the translational motion of the robot's body is being analyzed, assuming the lack of its inclination, slope and rotation. During the motion only a left and right side translation occurs, for the reason of keeping an appropriate dynamic balancing.

Therefore, equation (8) is simplified to:

$$\mathbf{0} = -\sum_k ({}^R\mathbf{r}_k \times {}^R\mathbf{F}_k) + {}^R\mathbf{r}_{\mathrm{CG}} \times m\,{}^R\mathbf{g}\,. \quad (9)$$

5.2. The ground reaction forces' distribution during single support phase

In the case of the single support phase, $k = s1$ ($s1 = L$ or $s1 = R$), i.e., only one vector of the ground reaction forces is unknown. It can be directly calculated from equation (7):

$${}^R\mathbf{R}_{s1} = -{}^R\mathbf{F}_{s1} = m\,{}^R\ddot{\mathbf{r}}_{CG} - m\,{}^R\mathbf{g}\,. \quad (10)$$

For the correctly designed dynamic balancing of the robot and a lack of unevenness of the ground, in the single support phase, the point at which the ground reaction force acts (the centre of pressure point) is also the zero moment point (on the basis of one of ZMP interpretations [8]), i.e.:

$${}^R\mathbf{r}_{s1} = {}^R\mathbf{r}_{\mathrm{ZMP}}\,. \quad (11)$$

5.3. The ground reaction forces' distribution during double support phase

In the case of double support phase, in equations (7) and (9) two unknown vectors of the ground reaction forces occur as well as two unknown vectors, which determine the points at which these forces act, but z component of the contact coordinates is known from geometry. Therefore in the given equations, 10 variables are unknown (6 components of the ground reaction forces and 4 coordinates of the points of contact).

In this connection, the definition of the additional four equations is necessary. Two additional equations result from the equilibrium of the ground reaction forces in reference to the zero moment point (on the basis of one of ZMP interpretations [8]), i.e.:

$${}^R F_{Zs1}({}^R x_{s1} - {}^R x_{\mathrm{ZMP}}) + {}^R F_{Zs2}({}^R x_{s2} - {}^R x_{\mathrm{ZMP}}) = 0\,, \quad (12a)$$

$${}^R F_{Zs1}({}^R y_{s1} - {}^R y_{\mathrm{ZMP}}) + {}^R F_{Zs2}({}^R y_{s2} - {}^R y_{\mathrm{ZMP}}) = 0\,, \quad (12b)$$

where: $s1$, $s2$ are accordingly the first and the second supported legs, while $s1 = L$ and $s2 = R$ or $s1 = R$ and $s2 = L$.

If the ground is not uneven, i.e., the foot touches the ground with its whole plane, ZMP is also the centre of pressure.

It has been assumed that the points of contact are translated in reference to Fk points, and these translations have been divided into 3 components:

$${}^R dx_k = {}^R x_k - {}^R x_{Fk},\ {}^R dy_k = {}^R y_k - {}^R y_{Fk},\ {}^R dz_k = -h_6, \quad (13)$$

where $k = \{L, R\}$.

In order to obtain an unequivocal result, the simplified assumptions are accepted, i.e., the directions of the points of contact translations during the double support phase are the same for both legs of the robot, i.e.:

$$\frac{{}^R dx_{s1}}{{}^R dy_{s1}} = \frac{{}^R dx_{s2}}{{}^R dy_{s2}} \quad (14)$$

and additionally they result from the direction of the resultant force, coming from the forces of gravity and inertia, so the following equations are true:

$$\frac{{}^R F_{Xk}}{{}^R F_{Zk}} = \frac{{}^R \ddot{x}_{\mathrm{CG}}}{{}^R \ddot{z}_{\mathrm{CG}} - {}^R g_Z},\quad \frac{{}^R F_{Yk}}{{}^R F_{Zk}} = \frac{{}^R \ddot{y}_{\mathrm{CG}}}{{}^R \ddot{z}_{\mathrm{CG}} - {}^R g_Z}\,. \quad (15)$$

The ground reaction forces, location of the points of contact of the feet, and their translation in reference to Fk points can be calculated using the selected equations (7), (9), (12)–(15).

Nevertheless, the result obtained is very complex and it is not suitable for the simulation tests due to singularities (in the denominators of some quantities, ${}^R z_{s1} - {}^R z_{s2}$ expression occurs, which in the typical case equals 0).

Therefore, in order to obtain the result in a proper form (simple and without any singularities), the process of calculating the results was divided into several stages. First of all, the vertical components of the ground reaction forces are determined, using, e.g., the second and the third equations of (7)[1], the second equation of (9) and equation (12b) in the following way:

$$
\begin{aligned}
{}^{R}F_{Zs1} &= \frac{m({}^{R}\ddot{z}_{\mathrm{CG}} - {}^{R}g_{Z})({}^{R}y_{\mathrm{ZMP}} - {}^{R}y_{Fs2})}{{}^{R}y_{Fs1} - {}^{R}y_{Fs2}}, \\
{}^{R}F_{Zs2} &= \frac{m({}^{R}\ddot{z}_{\mathrm{CG}} - {}^{R}g_{Z})({}^{R}y_{Fs1} - {}^{R}y_{\mathrm{ZMP}})}{{}^{R}y_{Fs1} - {}^{R}y_{Fs2}}.
\end{aligned}
\tag{16}
$$

Next, one of the possible results for the x and y components of the ground reaction forces is calculated, using the first two equations of (7) and the last equation of (9) as well as equations (12a) and (15):

$$
\begin{aligned}
{}^{R}F_{Xk} &= \frac{{}^{R}\ddot{x}_{\mathrm{CG}}}{{}^{R}\ddot{z}_{\mathrm{CG}} - {}^{R}g_{Z}}\ {}^{R}F_{Zk}, \\
{}^{R}F_{Yk} &= \frac{{}^{R}\ddot{y}_{\mathrm{CG}}}{{}^{R}\ddot{z}_{\mathrm{CG}} - {}^{R}g_{Z}}\ {}^{R}F_{Zk},
\end{aligned}
\tag{17}
$$

where k is notation of the supported leg ($k = \{L, R\}$).

Translation of the contact points can be calculated, depending on translation ${}^{R}dx_{s1}$ using equations (12a), (14) and the first of equations (13):

$$
{}^{R}dx_{s2} = -\frac{{}^{R}F_{Zs1}({}^{R}x_{Fs1} - {}^{R}x_{\mathrm{ZMP}} + {}^{R}dx_{s1}) + {}^{R}F_{Zs2}({}^{R}x_{Fs2} - {}^{R}x_{\mathrm{ZMP}})}{{}^{R}F_{Zs2}}. \tag{18}
$$

Substituting:

$$
{}^{R}dx_{s1} = -\frac{{}^{R}F_{Zs1}({}^{R}x_{Fs1} - {}^{R}x_{\mathrm{ZMP}}) + {}^{R}F_{Zs2}({}^{R}x_{Fs2} - {}^{R}x_{\mathrm{ZMP}})}{2\,{}^{R}F_{Zs1}} \tag{19}
$$

the final result is obtained:

$$
{}^{R}dx_{k} = -\frac{{}^{R}F_{Zs1}({}^{R}x_{Fs1} - {}^{R}x_{\mathrm{ZMP}}) + {}^{R}F_{Zs2}({}^{R}x_{Fs2} - {}^{R}x_{\mathrm{ZMP}})}{2\,{}^{R}F_{Zk}}, \tag{20a}
$$

$$
{}^{R}dy_{k} = -\frac{{}^{R}F_{Ys1}\,{}^{R}z_{s1} + {}^{R}F_{\mathrm{Ys2}}\,{}^{R}z_{s2} + {}^{R}F_{Zs1}\,{}^{R}y_{Fs1}}{2\,{}^{R}F_{Zk}} + \frac{{}^{R}F_{Zs2}\,{}^{R}y_{Fs2} + m\,{}^{R}g_{Z}\,{}^{R}\ddot{y}_{\mathrm{CG}}}{2\,{}^{R}F_{Zk}}, \tag{20b}
$$

[1] Equations (1)–(5) are the vector equations. Each corresponds to three scalar equations.

where k is notation of the leg ($k = \{L, R\}$).

The result obtained in this way is one of the possible ones.

5.4. Forces of the springs' reaction

The feet of the robot are equipped with springs. The relationship between deformation of the spring and the reaction force is taken as:

$$
R_j = \begin{cases} 0 & \text{for } h_j = h_{\max}, \\ k_S(h_{\max} - h_j) & \text{for } h_{\min} < h_j < h_{\max}, \\ R_{Zj} - m_6 g_Z & \text{for } h_j = h_{\min}, \end{cases} \tag{21}
$$

where: $k_S \approx 300$ [N/m] – stiffness of the spring, j – notation of the leg ($j = \{L, R\}$) – supported or transferred, R_j – force carried by the spring, h_j – height of the foot, $h_{\min} = 0.039$ [m], $h_{\max} = 0.049$ [m] – minimum and maximum heights of the foot, corresponding accordingly to the minimum and maximum deformation of the spring.

It is assumed that a given foot of the robot is in the support phase, if the deformation of the spring is maximal, i.e., if $R_j \geq R_{\min} = k_S(h_{\max} - h_{\min}) = 3$ [N].

The dependence given by (21) refers to any phase of the j leg movement.

5.5. Condition of avoiding slippage

The minimum acceptable values of the sliding friction coefficients for cooperation of the robot's feet with the ground are calculated on the basis of the following dependence:

$$
\mu_k = \sqrt{F_{Xk}^2 + F_{Yk}^2} \,/\, |F_{Zk}|. \tag{22}
$$

Dependence (22) represents the support phase of a given leg. In the case of the transfer phase, the minimum value of the sliding friction coefficient equals 0.

6. Simulation tests and animation of robot's motion

In order to verify the methods developed to generate the robot's motion as well as to analyse the ground reaction forces' distribution, simulation tests were performed, whose results are presented in this paper. The simulation was done using Matlab/Simulink package.

Due to the transformation of the joint angles recorded during human walk into angles and angular velocities of the robot's joints, time frames presented in figure 4 were obtained. Maximum angular velocities occurred in the knees and were close to 200 [°/s].

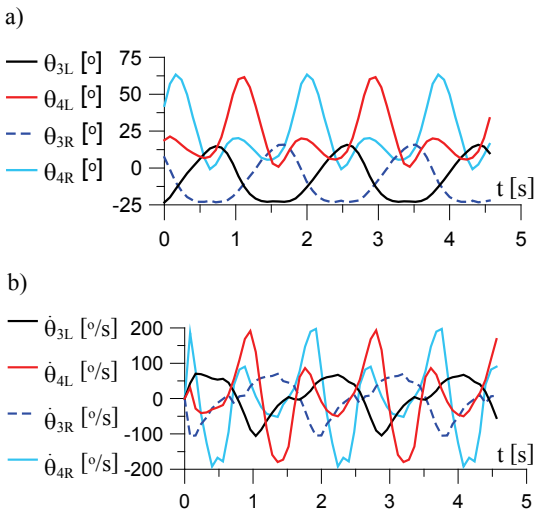

Fig. 4. Angles and angular velocities in the robot's joints obtained as a result of transformation of the joint angles recorded during human walk

Time frames of the x and y coordinates of F points for the left and right legs, in the reference frame connected with the robot's body, in the case of lack of balancing, are shown in figure 5.

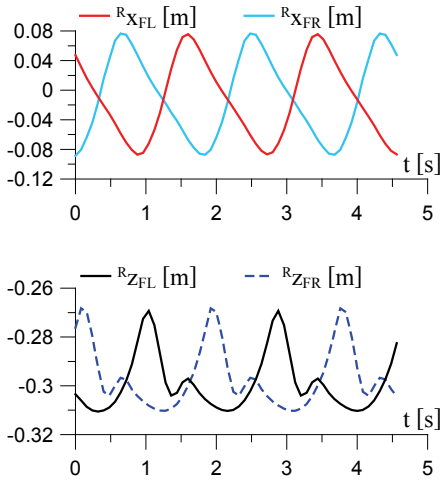

Fig. 5. Time frames of the x and y coordinates of F points for left leg and right leg, in the reference frame connected with the robot's body, in the case of a lack of balancing

The phases of the robot's motion related to the transfer and support indentified on the basis of coordinates of the Fj points are presented in figure 6. Value 0 denotes the support phase, value 1 the transfer phase of a given leg.

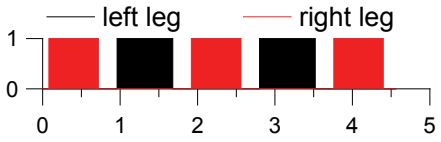

Fig. 6. Phases of the legs' motion: 0 – support, 1 – transfer

Figure 7a presents the motion trajectory of the right leg. Time frames shown in figure 5 as well as the motion trajectory of the FR point from figure 7a were initially determined, with the assumed lack of balancing ($\theta_{2j} = \theta_{6j} = 0$). As a result of the dynamic balancing of the robot, the motion trajectory of the Fj points was modified (figure 7b). Before the implementation of the balancing ${}^{R}y_{Fj}$ the coordinates of the Fj points were constant and equalled $d_0/2$, whereas after the implementation of the balancing, they have the form shown in figure 8.

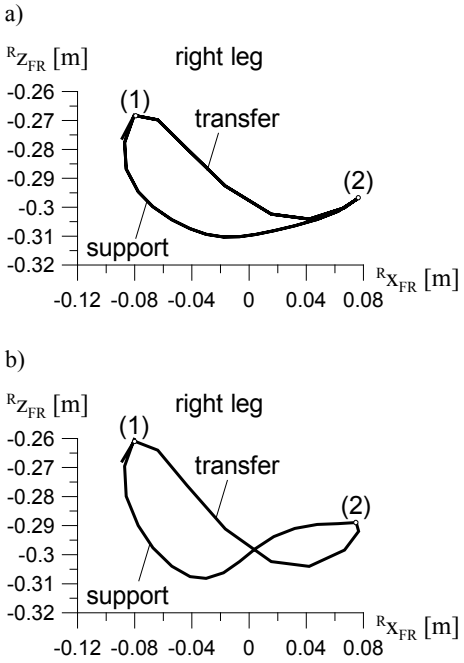

Fig. 7. Motion trajectories of the FR point of the right leg in the xz plane of the reference frame connected with the robot's body in the case of a lack of balancing (a), and with balancing (b)

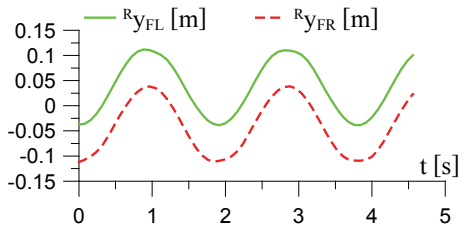

Fig. 8. Trajectories of the y coordinates of the F points of the left leg and right leg in the reference frame connected with the robot's body after implementation of the balancing

The trajectories obtained as a result of the calculation of the robot's centre of gravity and zero moment point coordinates are shown in figure 9.

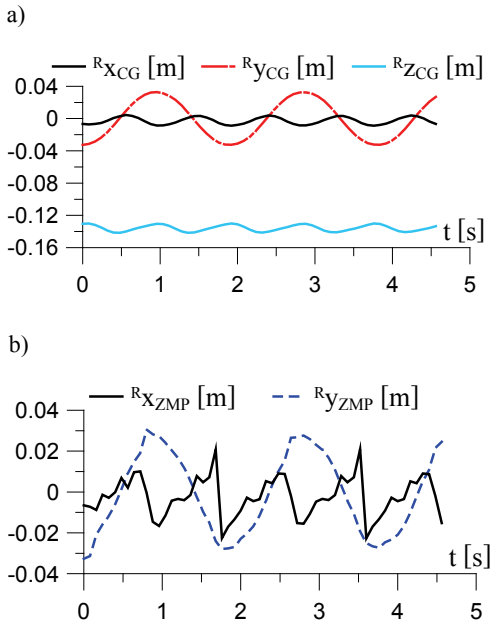

Fig. 9. Time frames of the robot's centre of gravity (a) and zero moment point coordinates (b) in the reference frame connected with the robot's body

A comparison of the obtained time frames of ZMP (figure 9b) with robot's motion phases and *Fj* points' coordinates proves the assumption that the maximum inclination of the robot occurs in the middle of the double support phase and that it is directed towards the leg, which will in a moment be the only one supported. At the maximum inclination of the robot the $^{R}y_{ZMP}$ coordinate is close to ±30 [mm], $^{R}y_{Fj}$ equals ca. ±40 [mm], and at the translation d_5 = ±9 [mm], which results in zero moment point to be located within the foot. The $^{R}y_{Fj}$ coordinates are moderately changing into the opposite ones during the transfer of the legs. The fastest change of the $^{R}x_{Fj}$ coordinates occurs in the double support phase. In the single support phase, these coordinates change moderately.

As a result of the simulation, the trajectories of the movement of the *R* and *FL* points in the absolute reference frame were obtained, as it is presented in figure 10.

During robot's motion the coordinate from *R* point changes within the small range (by ca. 20 [mm]), the length of the robot's step equals ca. 300 [mm], and the height of the foot elevation comes to the maximum level just after initialization of trasferring the leg, and equals ca. 30 [mm].

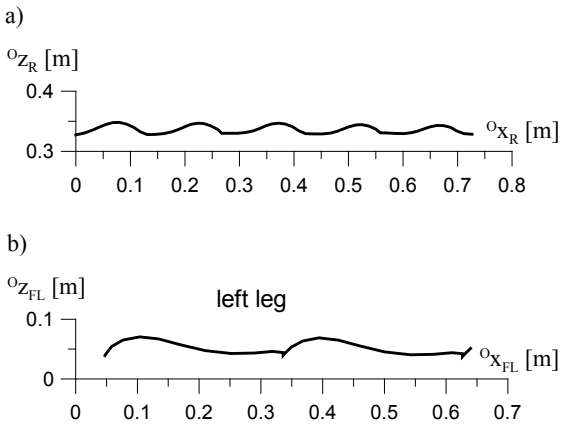

Fig. 10. Trajectories of movement of the *R* (a) and *FL* (b) points of the left leg in the non-moving reference frame

The components of the ground reaction forces' distribution during robot's walk, as determined during the simulation, are shown in figure 11. It should be noted that only one solution for the vertical components of the ground reaction forces' distribution is unequivocal. In the case of other quantities, obtaining one of the available results is possible by applying dependencies (17) and (20). Only the experimental tests can enable us to determine, which solution is typical of the robot's walk.

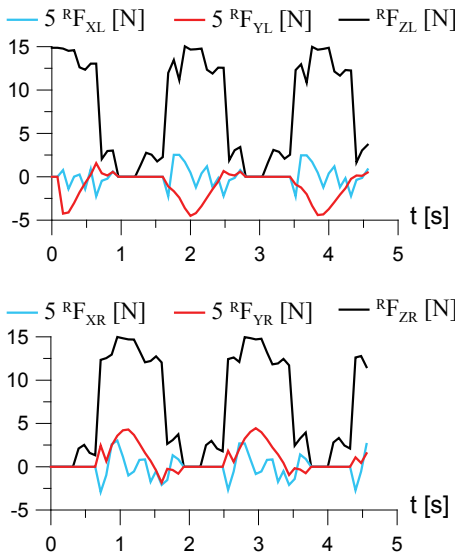

Fig. 11. Components of the ground reaction forces during robot's walk

Concurrently to the simulation tests the animation of the robot's motion was done using the Simulink 3D Animation Toolbox of Matlab/Simulink package. This Toolbox allows us to realistically create the 3D animations and to set the motion of the system during the simulation. This enables the easier understanding

of the designed system operation, as well as its real time testing, by additionally applying the Real Time Windows Target Toolbox. With the use of VR Sink block it is possible to define, e.g., what elements of the robot will be driven as well as to set both translations and rotations. During the animation, which is shown in a separate window, it is possible to manipulate the animated scene, including switching between defined views from different cameras. By using the Simulink 3D Animation Toolbox, simple physical models can be animated as well as the complex ones, which can be designed with software applications such as 3DStudio Max or AutoCAD. Also navigation with joystick is available.

The following data were essential for the animation: R point of the body coordinates in the absolute reference frame, body orientation and joint angles θ_{ij}. Two examples of the views of the robot during the animation (accordingly front view and right side view) are shown in figure 12. During the animation also the movement of the robot's centre of gravity was illustrated as well as the zero moment point.

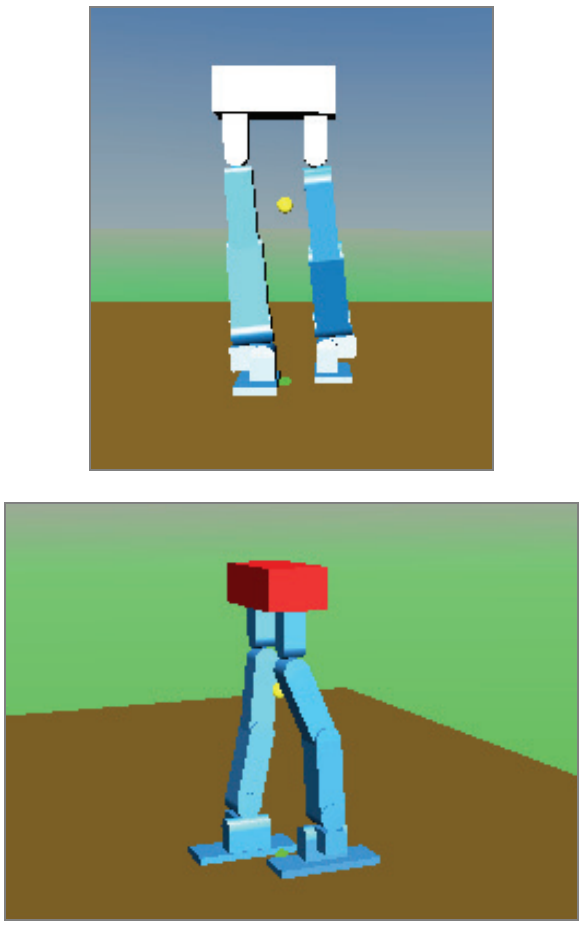

Fig. 12. Animation of the robot's motion, using the Simulink 3D Animation Toolbox of Matlab/Simulink package

7. Summary and further research

This paper presents the method for generating the biped robot's motion, based on the recorded human gait. The data recorded were adjusted to the robot's construction, and the missing quantities were complemented to ensure the dynamic balancing of the robot.

The method for determining the ground reaction forces' distribution during the dynamically stable walk of the biped robot has been presented. After denotating the essential equations, resulting from the robot's motion, as well as simplifying the assumptions taken, the symbolic values of the ground reaction forces' components have been determined as well as the coordinates of the conventional points of contact. Also the dependence, resulting from applying the springs within the robot's feet, was presented as well as the condition of avoiding the slippage.

The results of the study were proved by the simulation and animation of the robot motion performed with the support of the Matlab/Simulink package and Simulink 3D Animation Toolbox, which has verified the methods proposed.

The research presented demonstrated a designed forward motion of the robot. Further research will be focused on the realisation of the transition phases (e.g., change of the walking manner) as well as on the curvilinear motion trajectories. The research will require the application of the new data of the recorded human gait, or the development of such movements making use of synthesis, based partially on the previous data of the actual gait. The parametrization of the time frames obtained can be the first stage of such a research, which can be followed with making them dependent on the length and height of the walk as well as θ_{1j} angles of the feet rotation.

Also θ_{5j} angles, connected with the feet inclination, require modification, as in the double support phase the ${}^{R}z_{Fj}$ coordinates of the Fj points of both robot's feet, in the reference frame connected with its body, differ from each other. This is connected with the fact that during the backward step human foot is supported on the toes, and during the forward step on the heel. The slope of the robot's body or additional modification of the θ_{3j} angles in robot's hips (to avoid such a slope) can be the consequence of the above described modification.

In order to further verify the accuracy of the method presented, a simulation of the robot's dynamics can be performed with the application of a specialized software package (e.g., Adams).

Acknowledgements

The authors gratefully acknowledge the support for this work from Warsaw University of Technology Research Program and the Ministry of Scientific Research and Information Technology, Grant N N514 297935.

References

[1] *ASIMO – Technical Information*, American Honda Motor Co., Inc., Corporate Affairs & Communications, 2003 (www.honda.com).

[2] KIM J.-Y., PARK I.-W., OH J.-H., *Walking control algorithm of biped humanoid robot on uneven and inclined floor*, Journal of Intelligent and Robotic Systems, 2007, Vol. 48, No. 4, 457–484.

[3] LIM H., TAKANISHI A., *Compensatory motion control for a biped walking robot*, Robotica, 2005, Vol. 23, 1–11.

[4] LIM H., SETIAWAN S.A., TAKANISHI A., *Balance and Impedance Control for Biped Humanoid Robot Locomotion*, Proceedings of the 2001 IEEE/RSJ International Conference on Intelligent Robots and Systems, Maui, Hawaii, USA, Oct. 29–Nov. 03, 2001, 494–499.

[5] MITOBE K., CAPI G., NASU Y., *A new control method for walking robots based on angular momentum*, Mechatronics, 2004, 14, 163–174.

[6] VUNDAVILLI P.R., PRATIHAR D.K., *Soft computing-based gait planners for a dynamically balanced biped robot negotiating sloping surfaces*, Applied Soft Computing, 2009, 9, 191–208.

[7] MOUSAVI P.N., NATARAJ C., BAGHERI A., ENTEZARI M.A., *Mathematical simulation of combined trajectory paths of a seven link biped robot*, Applied Mathematical Modelling, 2008, 32, 1445–1462.

[8] VUKOBRATOVIĆ M., BOROVAC B.V., *Zero-Moment Point – thirty five years of its life*, International Journal of Humanoid Robotics, 2004, Vol. 1, No. 1, 157–173.

[9] ZIELIŃSKA T., *Maszyny kroczące. Podstawy, projektowanie, sterowanie i wzorce biologiczne*, PWN, Warszawa, 2003.

[10] ZIELINSKA T., CHEE-MENG CH., KRYCZKA P., JARGILO P., *Robot Gait Synthesis using the scheme of human motion skills development*, Mechanism and Machines Theory, Elsevier, 2008, 2008.09.07.

[11] HIRUKAWA H., KANEHIRO F., KAJITA S., FUJIWARA K., YOKOI K., KANEKO K., HARADA K., *Experimental Evaluation of the Dynamic Simulation of Biped Walking of Humanoid Robots*, Proceedings of the 2003 IEEE International Conference on Robotics & Automation, Taipei, Taiwan, September 2003, 14–19.

[12] KAJITA S., NAGASAKI T., KANEKO K., YOKOI K., TANIE K., *A Running Controller of Humanoid Biped HRP-2LR*, Proceedings of the 2005 IEEE International Conference on Robotics and Automation, Barcelona, Spain, April 2005, 618–624.

[13] KAJITA S., NAGASAKI T., KANEKO K., YOKOI K., TANIE K., *A Hop towards Running Humanoid Biped*, Proceedings of the 2004 IEEE International Conference on Robotics & Automation, New Orleans, LA, April 2004, 629–635.

[14] ANDERSON S.O., WISSE M., ATKESON C.G., HODGINS J.K., ZEGLIN G.J., MOYER B., *Powered Bipeds Based on Passive Dynamic Principles*, Proceedings of 2005 5th IEEE-RAS International Conference on Humanoid Robots.

[15] ZHOU D., LOW K.H., ZIELIŃSKA T., *An efficient foot-force distribution algorithm for quadruped walking robots*, Robotica, 2000, Vol. 18, 403–413.

[16] ZIELIŃSKA T., TROJNACKI M., *Synthesis of dynamical stable diagonal gait of a quadruped robot. Theoretical considerations* (1), (in Polish), Pomiary Automatyka Robotyka, 2007, 11, 5–11.

[17] ZIELIŃSKA T., TROJNACKI M., *Dynamical approach to the diagonal gait synthesis: theory and experiments*, Journal of Automation, Mobile Robotics & Intelligent Systems, 2009, Vol. 3, No. 2, 3–7.

[18] ZIELIŃSKA T., TROJNACKI M., *Postural stability in symmetrical gaits*, Acta of Bioenginering and Biomechanics, 2009, Vol. 11, No. 2, 57–64.

[19] KRYCZKA P., CHEE-MENG Ch., *The Design of a Humanoidal Biped for the Research on the Gait Pattern Generators*, Advances in Climbing and Walking Robots, Ming Xie at al. (editors), World Scentific, 2007, 435–444.

[20] KRYCZKA P., *An anthropomorphic biped: prototype and control system*, Bachelor's thesis, Warsaw University of Technology, Warsaw, 2007.

[21] CRAIG J.J., *Introduction to Robotics: Mechanics and Control*, 2nd Edition, Pearson/Prentice Hall, 2005.